I&EC research
Industrial & Engineering Chemistry Research

Article

pubs.acs.org/IECR

Simplified Methodology for the Design and Optimization of Thermally Coupled Reactive Distillation Systems

Fernando Israel Gómez-Castro,[†,‡] Vicente Rico-Ramírez,*[,†] Juan Gabriel Segovia-Hernández,[‡] Salvador Hernández-Castro,[‡] Guillermo González-Alatorre,[†] and Mahmoud M. El-Halwagi[§]

[†]Departamento de Ingenieria Quimica, Instituto Tecnologico de Celaya, Avenida Tecnologico y Garcia Cubas S/N, Celaya, Guanajuato, Mexico 38010

[‡]Departamento de Ingenieria Quimica, Division de Ciencias Naturales y Exactas, Universidad de Guanajuato, Campus Guanajuato, Noria Alta S/N, Guanajuato, Guanajuato, Mexico 36050

[§]The Artie McFerrin Department of Chemical Engineering, Texas A&M University, College Station, Texas, 77843-3122, United States

ABSTRACT: New intensified schemes have been recently proposed as an attempt to reduce energy requirements and equipment costs in reaction−separation processes. A design methodology for thermally coupled reactive distillation systems is proposed in this work. To design the columns, a method based on the Fenske−Underwood−Gilliland (FUG) equations is proposed and tested. The FUG equations, the mass and energy balances, and the phase equilibrium equations are used to formulate the model of the intensified systems. Such a model is then solved as a nonlinear programming problem; the objective function is the minimization of the heat duty in the column. Biodiesel production through the esterification of oleic acid with supercritical methanol is used as a case study. Results show the feasibility of obtaining designs with low energy requirements by using the proposed methodology. Because of nonconvexities present in the formulation, the estimated interlinking flows for the reactive Petlyuk column might not correspond to a minimum for energy requirements. Nevertheless, the resulting designs not only show low heat duties, with a difference of less than 2% from that minimum, but also have the capacity of achieving the desired conversion and purities.

1. INTRODUCTION

Recent research efforts in the development of production processes show an increasing concern for the reduction of environmental impact due to human activity. In those approaches, process intensification plays an important role. Process intensification is an area of chemical engineering whose main goal is finding production alternatives with low energy requirements, contaminant emissions, and cost. To achieve that goal, strategies including multitask equipment and process integration have been proposed. The basic structure of most of the production processes consists of a vessel where a chemical reaction takes place, consuming reactants and producing one or more desired products and some undesired byproduct, followed by a separation train. The most widely used separation process is distillation, because there is a lot of knowledge about its design and dynamic performance. Nevertheless, distillation has an inherent low thermodynamic efficiency (or second law efficiency, which represents the portion of the total energy entering the system which is actually used to perform the separation) which derives into high energy requirements for this operation. For distillation trains, attempts have been made to enhance the separation efficiency and, as a consequence, reduce their energy requirements. Thermal coupling is among these approaches. The increase of the thermodynamic efficiency when thermal coupling is incorporated depends on the nature of the mixture,[1] but in general, thermally coupled systems have higher thermodynamic efficiencies than conventional distillation sequences.[2] Thermal coupling implies the use of column configurations to avoid remixing.[3] For ternary mixtures, there are three structures which have been widely studied: the Petlyuk column or fully thermally coupled sequence (FTCS, Figure 1a), the thermally coupled direct sequence (TCDS, Figure 1b), and the thermally coupled indirect sequence (TCIS, Figure 1c). It has been found that the thermally coupled systems can reduce energy requirements from 30 to 50% when compared with conventional sequences[4−8] and may show better dynamic properties than conventional systems.[9−12] Nevertheless, the physical implementation of the Petlyuk column is not convenient, because of the unfavorable pressure profile required for its operation. Instead, a thermodynamically equivalent scheme, known as a dividing wall column (DWC), has been used at pilot and industrial scales.[13,14] The DWC consists of a single shell with a metallic plate which divides the shell and redistributes the internal flows of the column (Figure 2), although nonwelded structures have been recently introduced.[13] Different control strategies for dividing wall columns have also been proposed.[15,16]

A system involving a distillation train and a reactor can be intensified by coupling the reaction and separation systems into a reactive distillation column. Since both processes take place in a single shell, the equipment costs of reactive distillation are reduced. There are some additional advantages of using reactive distillation: (i) it is possible to override the chemical

Received: February 18, 2011
Revised: July 5, 2012
Accepted: August 5, 2012
Published: August 6, 2012

dx.doi.org/10.1021/ie201397a | *Ind. Eng. Chem. Res.* 2012, 51, 11717−11730

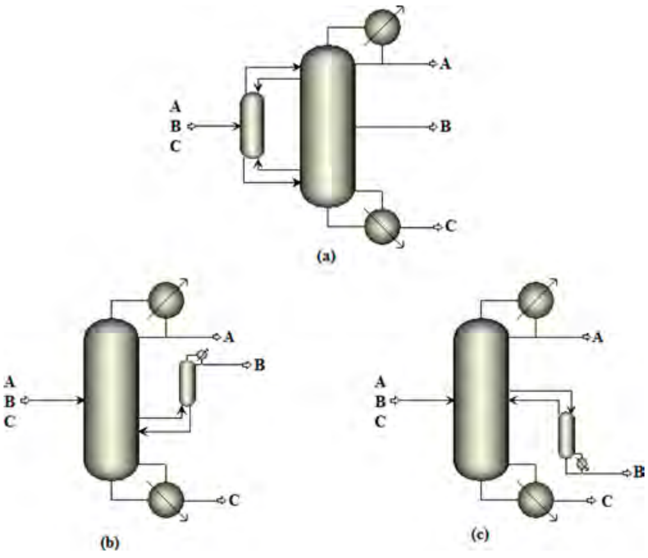

Figure 1. Thermally coupled distillation sequences: (a) Petlyuk column (FTCS); (b) thermally coupled direct sequence (TCDS); (c) thermally coupled indirect sequence (TCIS).

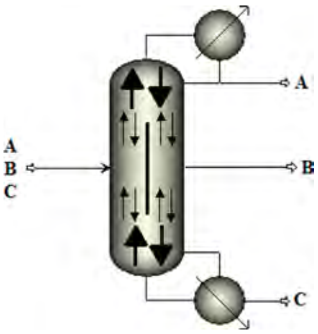

Figure 2. Simplified scheme of a dividing wall column.

equilibrium limitations, (ii) selectivity can be enhanced when multiple chemical reactions occur, and (iii) the global energy requirement is reduced when an exothermic reaction takes place because the heat released by the reaction can be used to vaporize products and/or byproducts.[17] Many products have been successfully produced in practice by reactive distillation, such as methyl acetate, fatty esters, methyl *tert*-butyl ether (MTBE), monoethylene glycol, and propylene oxide.[18]

Different design strategies have been proposed for reactive distillation. Some of these approaches consist of estimating composition changes for the simultaneous reaction and distillation processes.[19−26] Most of these graphical methods are useful when dealing with mixtures of up to four components. On the other hand, mathematical programming methods have been proposed for the design and optimization of reactive distillation columns, usually modeling the system as a mixed integer nonlinear programming (MINLP) problem.[27−31] The main advantage of such methods is that they obtain the optimal (or close to optimal) solution, depending mainly on the nature of the problem constraints. Even so, the mathematical and computational efforts required to reach such solutions are significant, and the use of integer variables makes this task even harder.[27] Furthermore, a very accurate initial guess of the solution is usually required to enhance the convergence of the system. When using nonderivative based methods, a good adjustment of the corresponding parameters is also required. Other approaches include the use of orthogonal collocation models to transform the mixed integer problem into an equivalent problem with continuous variables.[32−34]

Following the success of reactive distillation, reactive thermally coupled systems have been recently studied as an alternative for further reduction of fixed and variable costs in production processes. Barroso-Muñoz et al.[35] have proposed three different configurations to produce ethyl acetate: a reactive Petlyuk column, a reactive thermally coupled distillation system with a side rectifier, and a reactive thermally coupled distillation system with a side stripper. Mueller and Kenig[36] analyzed the reactive dividing wall column, which is thermodynamically equivalent to the reactive Petlyuk column, by using equilibrium and nonequilibrium stage models. The implementation of a reactive dividing wall column in a pilot plant has also been reported for the production of ethyl acetate.[37] Gomez-Castro et al.[38,39] have shown the feasibility of using a reactive Petlyuk column and a reactive thermally coupled direct sequence to produce biodiesel fuel with supercritical methanol. Other approaches have been proposed for using reactive distillation to produce fatty esters (biodiesel);[40−43] nevertheless, the use of reactive distillation in high temperature and pressure processes to produce biodiesel has not been extensively considered.

2. THERMALLY COUPLED REACTIVE DISTILLATION DESIGN

Most of the design approaches for thermally coupled reactive columns have been performed by a trial-and-error procedure, with the exception of the work of Kiss et al.,[17] where graphical methods are applied. Nevertheless, the use of graphical methods for mixtures with more than four components becomes difficult or infeasible. Thus, in this work a design methodology for the reactive dividing wall column (RDWC) and the reactive thermally coupled direct sequence (RTCDS) is proposed. The proposed approach considers mass and energy balances and the use of the Fenske−Underwood−Gilliland equations to determine the number of separation stages. Two solution strategies are considered. The first approach formulates the complete set of equations as a nonlinear programming (NLP) problem which intends to minimize the heat duty. The second strategy formulates only the mass and energy balances of the various sections of the column as an NLP problem, and then uses the Fenske−Underwood−Gilliland equations to calculate the remaining design variables, i.e., the number of stages, reflux ratio, and location of the interlinking streams.

The proposed methodology can be applied to reactive mixtures with any number of components, and it simplifies considerably the mathematical effort for the solution of the system of equations. Furthermore, it provides an estimate of the number of both nonreactive and reactive stages to achieve both the desired purities and the operating constraints. Results show that both of the design strategies are able to obtain feasible systems with lower energy requirements than that of the configuration reported by Gomez-Castro et al.[39] (assumed as initial guess).

3. MODELING EQUATIONS

Our model formulation for the design of the reactive thermally coupled systems includes mass balances, energy balances, phase equilibrium relationships, and the design equations.

3.1. Mass Balances.

Consider the reactive distillation column shown in Figure 3, with two feeds and three products.

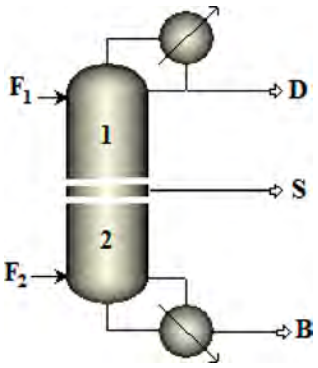

Figure 3. Reactive distillation column with two feeds and three product streams.

The column has a nonreactive section (section 1) and a reactive section (section 2), and from the delimiting tray of those two sections, a side stream is withdrawn. In the reactive section, a reversible chemical reaction, $\nu_A A + \nu_B B \leftrightarrow \nu_C C + \nu_D D$, occurs. A material balance for component i on the top of section k results in

$$d_{i,k} = \sum_j \mathrm{rec}_{d,i,j,k} z_{j,i} F_j - \left(\frac{\nu_i}{\nu_{rr}}\right) f_{\mathrm{conv}} \sum_j z_{j,rr} F_j \mathrm{rec}_{d,i,j,k} \qquad (1)$$

where $d_{i,k}$ is the flow of component i at the top of the section k, $\mathrm{rec}_{d,i,j,k}$ is the value of the recovery factor for component i at the top of section k from feed F_j, $z_{j,i}$ is the molar composition of component i in the feed stream F_j, ν_i is the stoichiometric coefficient for component i, ν_{rr} is the stoichiometric coefficient for a reference component r (which must be a reactant), and f_{conv} is the expected conversion; the value of f_{conv} can be assumed as the equilibrium conversion. In a similar way, a mass balance for component i at the bottom of section k results in

$$b_{i,k} = \sum_j \mathrm{rec}_{b,i,j,k} z_{j,i} F_j - \left(\frac{\nu_i}{\nu_{rr}}\right) f_{\mathrm{conv}} \sum_j z_{j,rr} F_j \mathrm{rec}_{b,i,j,k} \qquad (2)$$

Consider now the reactive Petlyuk column (RPC) shown in Figure 4. Mass balance equations, eqs 1 and 2, may also be applied to the main column of the RPC (sections 1 and 2), but the feed flow rate F_j must be replaced by a total feed flow rate F_{jT}, where

$$F_{1T} = F_1 + \mathrm{FV1} \qquad (3)$$

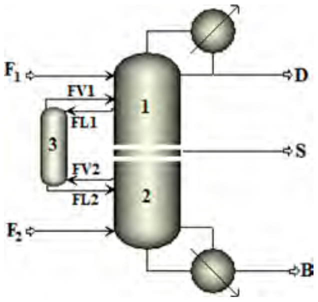

Figure 4. Section distribution for the mass balance in the RPC.

$$F_{2T} = F_2 + \mathrm{FL2} \qquad (4)$$

F_{1T} is the pseudofeed stream to section 1 of the main column, consisting of the fresh feed stream F_1 and the vapor stream FV1 leaving the prefractionator; similarly, F_{2T} is the pseudofeed stream to section 2 of the main column, consisting of F_2 and FL2. Mass balance equations can also be obtained for the prefractionator of the RPC (section 3) as follows (initial guesses for FL1 and FV2 are needed):

$$\mathrm{FV1} = f_{\mathrm{part}}(\mathrm{FL1} + \mathrm{FV2}) \qquad (5)$$

$$\mathrm{FL2} = (\mathrm{FL1} + \mathrm{FV2}) - \mathrm{FV1} \qquad (6)$$

where f_{part} is the partition factor. The partition factor represents the fraction of the total feed to the prefractionator which leaves that section as a vapor flow; its value must be determined by energetic considerations. The initial values for $\mathrm{rec}_{d,i,j,k}$, f_{part}, and f_{conv} are in fact unknown, but they can be estimated prior to the design procedure through rigorous simulations.[39] Nevertheless, since f_{part} is a decision variable directly related to the interlinking flows, its value is modified through the optimization strategy, as will be described later.

For the RTCDS, consider the system depicted in Figure 5. The mass balance equations for the main column are also given by eqs 1 and 2, but in the case of section 3, the total feed involves a pseudofeed stream composed by F_1 and FL. The material balance for the side rectifier is then given by eq 7:

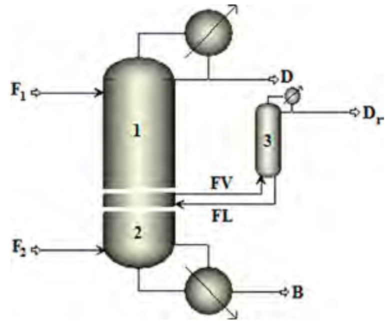

Figure 5. Section distribution for the mass balance in the RTCDS.

$$\mathrm{FL} = \mathrm{FV} - D_r \qquad (7)$$

3.2. Energy Balances.

Global energy balances are used to calculate the heat required to perform the separations. In the case of the RPC, the total amount of heat entering the main column ($Q_{\mathrm{ent,RPC}}$) is given by eq 8.

$$Q_{\mathrm{ent,RPC}} = h_{F_1}F_1 + h_{F_2}F_2 + h_{\mathrm{FV1}}\mathrm{FV1} + h_{\mathrm{FL2}}\mathrm{FL2} + Q_{\mathrm{rxn}} + Q_{\mathrm{reb}} \qquad (8)$$

In eq 8, h is the molar enthalpy of the stream, Q_{rxn} is the heat of reaction, and Q_{reb} is the thermal duty in the reboiler of the main column. The heat of reaction is calculated as follows:

$$Q_{\mathrm{rxn}} = h_{\mathrm{rxn},i}\left(\frac{\nu_i}{\nu_{rr}}\right) f_{\mathrm{conv}} z_{rr,F_1} F_1 \qquad (9)$$

where rr indicates the reference component for the reaction and $h_{\mathrm{rxn},i}$ is the molar enthalpy of reaction. Similarly, the total amount of heat leaving the main column ($Q_{\mathrm{out,RPC}}$) is

$$Q_{\mathrm{out,RPC}} = h_D D + h_S D + h_B B + h_{\mathrm{FL1}}\mathrm{FL1} + h_{\mathrm{FV2}}\mathrm{FV2} + Q_{\mathrm{COND}} \quad (10)$$

where Q_{COND} is the heat removed by the condenser and can be calculated as

$$Q_{\mathrm{COND}} = V\sum_{i=1}^{\mathrm{NC}} \lambda_i y_{\mathrm{Vd},i} \quad (11)$$

In eq 11 λ_i is the enthalpy of vaporization for component i, $y_{\mathrm{Vd},i}$ is the composition of component i in the vapor entering the condenser, and V is the flow rate for such a vapor stream. The reboiler duty is then calculated as

$$Q_{\mathrm{reb}} = Q_{\mathrm{out,RPC}} - (h_{F_1}F_1 + h_{F_2}F_2 + h_{\mathrm{FV1}}\mathrm{FV1} + h_{\mathrm{FL2}}\mathrm{FL2} + Q_{\mathrm{rxn}}) \quad (12)$$

Similarly, for the RTCDS, the heat entering the main column is computed as given by eq 13:

$$Q_{\mathrm{ent,RTCDS}} = h_{F_1}F_1 + h_{F_2}F_2 + h_{\mathrm{FL}}\mathrm{FL} + Q_{\mathrm{rxn}} + Q_{\mathrm{reb}} \quad (13)$$

The heat leaving the main column of the RTCDS is given by

$$Q_{\mathrm{out,RTCDS}} = h_D D + h_B B + h_{\mathrm{FV}}\mathrm{FV} + Q_{\mathrm{COND}} \quad (14)$$

Thus, the amount of energy required in the reboiler of the column is

$$Q_{\mathrm{reb}} = Q_{\mathrm{out}} - (h_{F_1}F_1 + h_{F_2}F_2 + h_{\mathrm{FL}}\mathrm{FL} + Q_{\mathrm{rxn}}) \quad (15)$$

3.3. Phase Equilibrium. Phase equilibrium calculations are needed to perform mass and energy balances. The thermodynamic models used and the number of phases involved will depend on the system under analysis. For instance, a phi−gamma ($\Phi-\gamma$) formulation can be used for vapor−liquid equilibrium calculations (VLE), although it is quite common to find three-phase mixtures (VLLE) in reactive distillation systems.

In the VLE case (which will be used later in our case study), the equilibrium constant and the activity coefficients of the $\Phi-\gamma$ formulation are given by[44]

$$K_{\mathrm{eq}} = \frac{y_i}{x_i} = \frac{\gamma_i P_i^{\mathrm{sat}}}{\Phi_i P} \quad (16)$$

where the activity coefficient has been calculated by using the NRTL model equations. The interaction parameters can be estimated through experimental data or through the help of a process simulator.

3.4. Design Equations. The use of the Fenske−Underwood−Gilliland (FUG) and the Kirkbride equations constitutes the classical approach for the design of conventional distillation columns by shortcut methods. A modified version of those equations is used in this work for the design of the thermally coupled reactive distillation systems; the modifications applied are described in section 4.

4. DESIGN STRATEGY

A modified version of the Underwood equations is used for the design of thermally coupled reactive distillation systems. This section provides the assumptions made in this work when applying the shortcut method based on the FUG and Kirkbride equations.

4.1. Minimum Reflux Ratio Calculation. To estimate the minimum reflux ratio, consider the flow distribution presented in Figure 6. It is assumed that the internal vapor and liquid molar flows for each subsection remain nearly constant, affected only by the feed streams. Sotudeh and Shahraki[45] have shown that, for a nonreactive Petlyuk column, the minimum vapor flow ($V_{\min}$) may occur in any of the different subsections into which the main column has been divided; the authors also suggest the selection of the higher value of $V_{\min}$ to make sure that the desired separation will take place. This result will be used for the RPC. Since the feed composition is required in the Underwood equation, compositions, flow rates, and liquid fractions of the pseudofeed streams need to be calculated for each section of the RPC. In the case of section 1, the pseudofeed stream considers both F_1 and FV1. The pseudofeed stream for section 2 includes F_2 and FL2. In the case of the prefractionator (section 3), FL1 and FV2 conform the pseudofeed stream, since there is no fresh feed stream entering this section. The liquid fractions of the different sections are given by

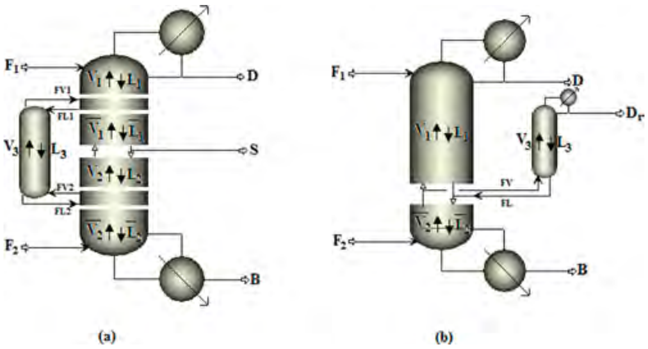

Figure 6. Flow distribution for the calculation of minimum reflux ratio: (a) reactive Petlyuk column; (b) reactive thermally coupled direct sequence.

$$q_{\mathrm{pf1,RPC}} = \frac{F_1}{F_1 + \mathrm{FV1}} \quad (17)$$

$$q_{\mathrm{pf2,RPC}} = \frac{F_2}{F_2 + \mathrm{FL2}} \quad (18)$$

$$q_{\mathrm{pf3,RPC}} = \frac{\mathrm{FL1}}{\mathrm{FL1} + \mathrm{FV2}} \quad (19)$$

where $q_{\mathrm{pf}k}$ is the liquid fraction of the pseudofeed stream in section k. It is now possible to calculate the minimum vapor flow for the different sections by considering the pseudofeed compositions and liquid fractions. Notice that there will be $n-1$ Underwood roots, so that the correct value of $V_{\min}$ for each section and for the whole RPC will be selected as suggested by Halvorsen et al.,[46] with a modification made to consider the pseudofeed stream in section 2:

$$V_{\min,1} = \max\{V_{\min,1}(\theta_1), V_{\min,1}(\theta_2), V_{\min,1}(\theta_3), V_{\min,1}(\theta_4)\} \quad (20)$$

$$\bar{V}_{\min,2} = \max\{\bar{V}_{\min,2}(\theta_1'), \bar{V}_{\min,2}(\theta_2'), \bar{V}_{\min,2}(\theta_3'), \bar{V}_{\min,2}(\theta_4')\} \quad (21)$$

$$V_{\mathrm{min,RPC}} = \max\{V_{\min,1}, \bar{V}_{\min,2} + (1 - q_{\mathrm{pf2}})F_{\mathrm{pf2}}\} \quad (22)$$

where θ_n and θ_n' are the *n*th Underwood roots for section 1 and section 2, respectively, $V_{\min,1}(\theta_n)$ is the minimum vapor flow in section 1 calculated with the Underwood root θ_n, $\bar{V}_{\min,2}(\theta_n')$ is the minimum vapor flow in section 2 calculated with the Underwood root θ_n', F_{pf2} is the molar flow rate of the pseudofeed stream in section 2, and $V_{\min,\mathrm{RPC}}$ is the minimum vapor flow for the reactive Petlyuk column.

Similar assumptions have been made for the calculation of $V_{\min}$ in the case of the RTCDS. Section 1 has only one feed stream (F_1), but a pseudofeed stream composed by F_2 and FL has been used in the case of section 2. The liquid fraction for this pseudofeed stream is given by

$$q_{\mathrm{pf2,RTCDS}} = \frac{\mathrm{FL}}{F_2 + \mathrm{FL}} \tag{23}$$

The values for the minimum vapor flow in sections 1 and 2 are given by eqs 20 and 21. For section 3 the resulting expression is given by eq 24.

$$V_{\min,3} = \max\{V_{\min,3}(\theta_1''), V_{\min,3}(\theta_2''), V_{\min,3}(\theta_3''), V_{\min,3}(\theta_4'')\} \tag{24}$$

where θ_n'' is the *n*th value of the Underwood root in section 3 of the RTCDS. Since there are two condensers in that configuration, there will also be two values of $V_{\min}$, one for the condenser of the main column and the other for the condenser of the side rectifier. Those values are estimated by using an approach similar to that presented for the reactive Petlyuk column:

$$V_{\min,\mathrm{RTCDS(MC)}} = \max\{V_{\min,1}, \bar{V}_{\min,2} + (1 - q_{\mathrm{pf2}})F_{\mathrm{pf2}}\} \tag{25}$$

$$V_{\min,\mathrm{RTCDS(SR)}} = V_{\min,3} \tag{26}$$

In eq 25, $V_{\min,\mathrm{RTCDS(MC)}}$ is the minimum vapor flow in the main column of the RTCDS, and in eq 26, $V_{\min,\mathrm{RTCDS(SR)}}$ is the minimum vapor flow in the side rectifier of the RTCDS.

4.2. Minimum and Actual Number of Stages. The minimum number of stages for each of the three main sections of an RDC is calculated through the Fenske equation in a way similar to that in the nonreactive case, which is a significant assumption and the main source of error in this approach. From mass balances, the compositions of both the distillate and the side stream are known. In the case of section 2 the compositions of the side stream and of the bottom are also known. For section 3 the required data are the vapor composition of the FV1 stream and the liquid composition of FL2; such data may also be estimated from the mass balances in the prefractionator. The relative volatilities can be evaluated as the geometric average of the relative volatilities at the top and bottom of each section.

In the case of the RTCDS, calculation of the minimum number of stages for section 1 can be performed by using the composition at the top of the main column and the composition of the liquid in equilibrium with the vapor stream FV. For section 2, the compositions used are those corresponding to FV and to the bottom of the main column. Finally, for the side rectifier, distillate compositions of section 3 and the liquid stream FL compositions are used.

Once the minimum number of stages has been calculated, the basic Gilliland equation (another source of error) is then used to estimate the actual number of stages. Since the actual reflux ratio is unknown, a factor "facrd" has been used to calculate it through the expression $R_{\mathrm{RPC}} = (\mathrm{facrd})R_{\min,\mathrm{RPC}}$. As an initial guess, this factor has been considered equal to 1.3. For the RTCDS, calculation of the actual number of stages is performed in a similar way, using the factors "facrdc" and "factdcsr" for the main column and the side rectifier, respectively.

4.3. Feed and Product Stages. The Kirkbride equation is used to estimate the feed stages (location of the interlinking streams). In order to design the reactive dividing wall distillation column (RDWC), interlinking streams FV1 and FL1 are enforced to be located on the same stage. The same constraint applies to FV2 and FL2. The stage distribution for the RPC is shown in Figure 7a. The numbers of stages N_2, N_3, N_4, and N_5 are computed by using the Kirkbride equation. The number of stages on the prefractionator (N_1) was calculated as the sum of N_3 and N_4, since those are the stages in which the dividing wall must be installed.

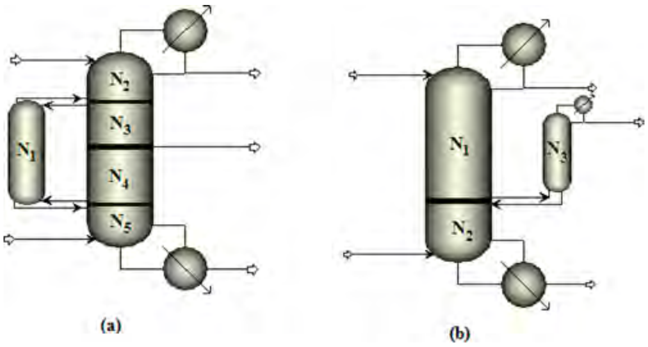

Figure 7. Stage distribution for the location of the interlinking flows: (a) reactive Petlyuk column; (b) reactive thermally coupled direct sequence.

In the case of the RTCDS, since the only interlinking stage is located on the boundary stages between sections 1 and 2, its location is implicitly determined by the Gilliland equation, as seen in Figure 7b. Thus, it is not necessary to use the Kirkbride equation for this system.

5. SOLUTION APPROACH

The design and optimization of the reactive thermally coupled systems is first posed as an NLP problem which intends to minimize the heat duty in the reboilers (external energy requirements on the column). The solution of the problem was obtained by using the CONOPT solver within GAMS. Clearly, the number of stages is an integer variable, but the solution is simplified through the FUG equations so it was assumed to be a continuous variable.

Two solution strategies were used. In the first one (method 1), the complete set of equations was solved as an NLP by using the design variables obtained in the literature[39] as initial values. The second approach (method 2) considers the simultaneous solution of only mass balances, energy balances, and equilibrium equations as an NLP problem, also aiming for the minimum energy requirement; the results obtained were then used to complete the calculations by applying the design equations with the optimal flows calculated through the NLP.

The degrees of freedom in the DWC are the partition factor in the prefractionator (f_{part}), the factor to calculate the actual reflux ratio (facrd), and the interlinking flow rates FL1 and FV2 for each component. In the case of the RTCDS, the degrees of freedom are the factor used to calculate the actual reflux ratio for the main column (facrdc) and the factor used to calculate the actual reflux ratio for the side rectifier (factdcsr).

In general, the optimization problem is represented as

$$\begin{aligned} &\min\ Q_{\text{reb}} \\ \text{s.t.}\quad & f(x) = 0 \\ & g(x) \geq 0 \end{aligned} \tag{27}$$

where Q_{reb} is the thermal duty for a given system, and $f(x)$ and $g(x)$ are the model constraints. The constraints include the mass and energy balances, the phase equilibrium equations, and the design equations for method 1 and the mass and energy balances and the phase equilibrium equations for method 2. Table 1 provides the decision variables for both of the thermally coupled systems under analysis. Most of the variables shown in Table 1 have a direct impact on the thermal requirements of the column. Notice that Table 1 also includes some factors used to calculate the main design variables: for instance, the actual reflux ratio is determined by the minimum reflux ratio and the reflux factors (facrd, facrdc, and factdcsr); likewise, the composition, molar flow rate, and temperature of the interlinking flows are determined by the partition factor (f_{part}).

Table 1. Decision Variables for the Design of Thermally Coupled Systems

RDWC
compositions of the interlinking streams
total molar flow of the interlinking streams
temperature of the interlinking streams
factor facrd for the calculation of actual reflux ratio
partition factor f_{part} (fraction of feed going to the prefractionator)
actual reflux ratio for the main column
number of stages in the prefractionator
number of stages for the nonreactive section in the main column
number of stages for the reactive section in the main column
RTCDS
compositions of the interlinking streams
total molar flow of the interlinking streams
temperature of the interlinking streams
factor facrdc for the calculation of actual reflux ratio
actual reflux ratio for the main column
factor factdcsr for the calculation of actual reflux ratio
actual reflux ratio for the side rectifier
number of stages for the nonreactive section in the main column
number of stages for the reactive section in the main column
number of stages in the side rectifier

Notice that the optimization model does not consider either the impact of investment costs in the optimal design or the ability of the column to compensate for variations in the activity of the reactions. It has been reported that the use of reactive thermally coupled distillation systems does not necessarily imply a significant increase in the investment costs.[47] Furthermore, not all of the thermal coupling schemes have the potential of being beneficial in terms of energy savings.[48] We could expect the investment cost effect to be negligible with respect to the utility costs (implicitly considered when minimizing the thermal duty), but the effect of the activity of the reaction needs to be further investigated.

Once the optimization strategy (and further sequential calculations in method 2) provides an estimation of the column configurations (parameters and design variables), a parametric search with respect to the main design variables is conducted by using a process simulator, in order to test and to improve the performance of the designs obtained by the shortcut method (in terms of energy requirements). The use of a process simulator with rigorous thermodynamic models and hydraulic equations allows consideration of the effect of parameters such as the reactive stage holdup, which is neglected by simplified designs based on shortcut methods. Notice that, instead of using the reactive stage holdup (which implies a stage-by-stage calculation), in our shortcut method we propose to incorporate the reaction into the analysis through the estimation of the overall conversion of the reactive system; such conversion is then used in the mass balances. The estimation of the overall conversion will of course have to consider any information regarding kinetics expressions which are consistent with the reactants involved. The complete design methodology in both cases is depicted in Figure 8.

6. CASE STUDY

The reactive system studied involves biodiesel production by the Saka–Dadan method.[49] In particular, it consists of the esterification of oleic acid with supercritical methanol to produce methyl oleate, as described by Gomez-Castro et al.[38,39] The chemical reaction proceeds as indicated by eq 28:

$$\text{OLAC} + \text{MeOH} \leftrightarrow \text{MeOL} + \text{H}_2\text{O} \tag{28}$$

where OLAC stands for oleic acid, and MeOH, MeOL, and H_2O represent methanol, methyl oleate, and water, respectively. Notice that 1 mol of methyl oleate is produced for each mole of oleic acid used as reactant. When using eq 9, oleic acid (OLAC) is the reference component for the reaction and, therefore, $h_{\text{rxn},i}$ has been calculated for i = OLAC as 41 573.23 kJ/kmol.

Esterification takes place at 7 MPa and 270 °C.[50] The reaction is reversible; however, the reverse reaction effects are small and a yield higher than 90% can be obtained.[49] The analyzed system includes the four components involved in the reaction (OLAC, MeOH, MeOL, and H_2O) as well as a small amount of glycerol remaining from the two-phase separation previous to the esterification step.[39] It has been reported that, given the pressure and temperature conditions, the esterification reaction occurs in a single liquid phase;[49,51] thus only vapor–liquid equilibrium (VLE) calculations are considered for the phase equilibrium. The compositions for the two feed streams are presented in Table 2. VLE calculations were performed through the $\Phi-\gamma$ model as described by eqs 16–19. Interaction parameters were obtained from the Aspen One process simulator and are given in Table 3. The parameter C_{ij} is always assumed as 0.3.The fatty acid rich stream contains water and glycerol, whereas the methanol feed contains pure methanol. Both feed streams enter the system at 7 MPa and 270 °C. The flow rate of the fatty acid feed stream is 267.58 kmol/h; the methanol feed is 412.69 kmol/h.

7. RESULTS AND DISCUSSION

Before the main results of our approach are discussed, the following section provides a summary of the simplifying assumptions made to complete the design procedure for our case study.

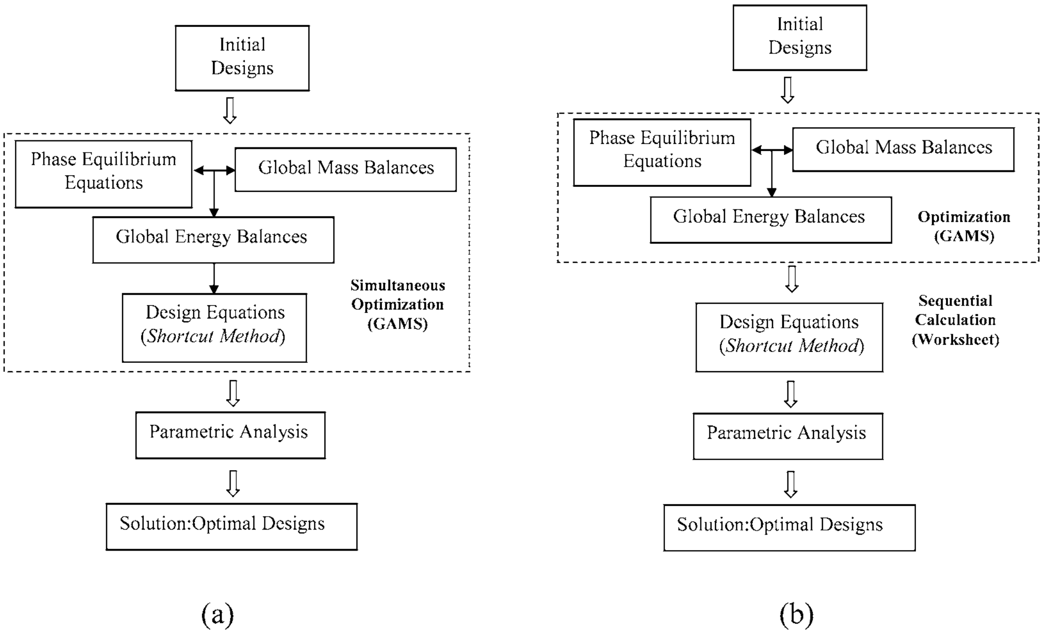

Figure 8. Design methodology: (a) method 1; (b) method 2.

Table 2. Compositions of the Feed Streams (mol %)

component	fatty acid feed	methanol feed
MeOH	0.0000	1.0000
H_2O	0.4825	0.0000
GLI	0.0035	0.0000
OLAC	0.5139	0.0000
MeOL	0.0000	0.0000

7.1. Summary of Simplifying Assumptions. The following is a list of the main assumptions made to design the thermally coupled reactive configurations applied to the case study:

1. The esterification reaction occurs in a single liquid phase.[49,51]
2. Vapor–liquid equilibrium can be represented using a $\Phi-\gamma$ formulation.
3. The location of the methanol feed stream and the oleic acid feed stream is fixed at the bottom and top of the main column, respectively.
4. The pressure remains almost constant at 7 MPa across the main columns of the thermally coupled reactive configurations.
5. Sections with two feed streams are assumed as having a single pseudostream with the purpose of performing calculations for minimum reflux and minimum number of stages.
6. The side stream on the main column of the RDWC is located on the boundary region between the nonreactive section and the reactive section.
7. The interlinking stream on the main column of the RTCDS is located on the boundary region between the nonreactive section and the reactive section.
8. All of the variables involved in the optimization strategy are assumed to be continuous.

Further, notice that the presence of nonideal conditions (such as the existence of azeotropes) complicates any approach to the design of reactive separation systems. We believe, however, that the boundaries imposed for those nonideal conditions can be considered a priori on a case-by-case basis, so

Table 3. Binary Interaction Parameters for the NRTL Equation

A_{ij}					
component	MeOH	H_2O	GLI	MeOL	OLAC
MeOH	0.0000	−2.6260	0.0000	0.0000	0.0000
H_2O	4.8241	0.0000	−1.0937	0.0000	0.0000
GLI	0.0000	−0.7026	0.0000	0.0000	0.0000
MeOL	0.0000	0.0000	0.0000	0.0000	0.0000
OLAC	0.0000	0.0000	0.0000	0.0000	0.0000
B_{ij}					
component	MeOH	H_2O	GLI	MeOL	OLAC
MeOH	0.0000	828.3871	559.8946	997.3854	662.8329
H_2O	−1329.5435	0.0000	226.6530	5916.0432	4978.8569
GLI	−221.4105	157.4594	0.0000	2684.4196	1804.7939
MeOL	66.9798	930.1429	2255.1778	0.0000	255.5463
OLAC	−182.3177	537.2737	1100.3134	−132.5211	0.0000

the existence of azeotropes can be predicted before using any design methodology through rigorous simulation or by reactive residual curves. For the case study under consideration, there are no physical or reactive azeotropes reported. In our work, rigorous simulations were performed before the optimization procedure. If an azeotrope is predicted or is known to exist in some other system, its presence will affect the maximum possible recovery, which is a parameter involved in the design strategy that we proposed here.

7.2. Results. The column configurations obtained from both of the solution methods are presented in Table 4 for the RDWC. Method 1 is the simultaneous solution of the whole system of equations, whereas method 2 corresponds to the solution of the mass and energy balances and the posterior design of the column. In Table 4, N_{pre} is the number of stages on the prefractionator, $N_{MC,calc}$ is the number of stages on the main column as calculated, and $N_{MC,total}$ is the total number of stages in the main column, including the condenser and the reboiler. For the calculation of the feed stage in the main column of the RDWC, the fatty acid feed F_1 has been located in stage 2 and the methanol feed is located at the bottom of the column. Those decisions were made in our case study because any other configuration of those two feed streams causes failure on the mass balances and drying of the stages on the columns for both systems.[38,39]

Table 4. Designs Obtained from the Two Solution Methods, RDWC

	method 1	method 2
N_1	5	4
N_2	3	3
N_3	3	3
N_4	2	1
N_5	1	2
N_{pre}	5	4
$N_{MC,calc}$	9	9
$N_{MC,total}$	11	11
N_{reac}	8–10	8–10
interlinking stages	4, 9	4, 8
side stream stage	7	7
R_{col}	1.027	1.214
FL1 (kmol/h)	14.982	6.214
FV2 (kmol/h)	62.813	76.185
$Q_{reb,sim}$ (kJ/h)	53 083 486.4	46 344 109.2

Those configurations were tested by simulations on Aspen One by assuming 99 mol % purity for water, 90 mass % purity for methyl oleate, and 91.33 mol % purity for methanol. The energy requirement provided in Table 4 corresponds to the results of the simulations.

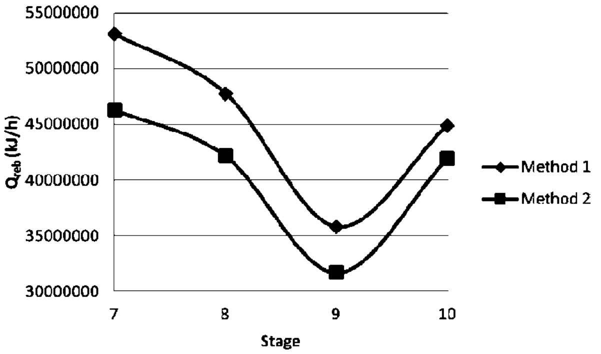

Figure 9. Variation of energy requirements with respect to changes in the side stream withdrawal stage (RDWC).

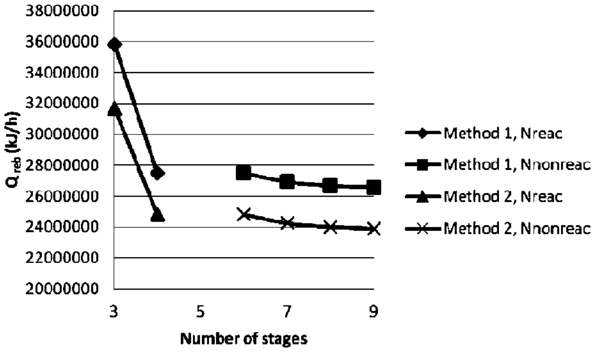

Figure 10. Variation of energy requirements with respect to changes in the numbers of reactive and nonreactive stages (RDWC).

After the design variables were estimated through the proposed approach, a sensitivity analysis was performed with respect to the main design variables to determine if the designs obtained are the systems with the lowest heat duty; otherwise, the analysis may suggest some modifications to the values of the design variables. In the analysis, a residence time of 0.3 h for all the reactive stages has been considered, as proposed in a previous work.[38] Changes in the heat duty when the location of the side stream is modified are shown in Figure 9. When the side stream is extracted from the reactive section (instead of the boundary zone between the nonreactive and reactive zones), the heat duty in the column is considerably reduced, passing through a minimum and then being increased as the side stream stage gets close to the bottom of the column. Moreover, Figure 10 provides an analysis of the effect of Q_{reb} when the numbers of reactive and nonreactive stages are increased. Incorporating one additional reactive stage to the initial configuration reduces heat duty, but when more reactive stages are added, no convergence is achieved for the purities specified; this problem is expected to occur, since shortcut models more easily satisfy product specifications than rigorous models. When more nonreactive stages are used, a decrease in the thermal duty is observed, but that reduction is not as significant as the one observed when the number of reactive stages is increased. Optimization curves for the interlinking flows are presented in Figure 11a for the design obtained by method 1 and in Figure 11b for the design obtained by method 2. The initial values correspond to the interlinking flow rates as calculated by the optimization methodology. When the interlinking flow rate is changed, a decrease in heat duty is achieved, but this reduction is minimal (less than 1% relative to the initial value). Thus, the initial values for the interlinking flow rates are used for the final configurations. After studying the results from the design strategy and the sensitivity analysis, the final values for the design variables for the RDWC were selected and are provided in Table 5. Simulations for a reactive distillation column (RDC1) with a side stream were performed for comparison purposes; the RDC1 has the same number of stages as the main column of the RDWC. The results for the RDC1 are also included in Table 5. The design of the RDWC obtained by method 2 (RDWC2) has the lowest heat duty among the three systems, and even the RDC1 has lower energy requirements than the RDWC designed by method 1 (RDWC1). Never-

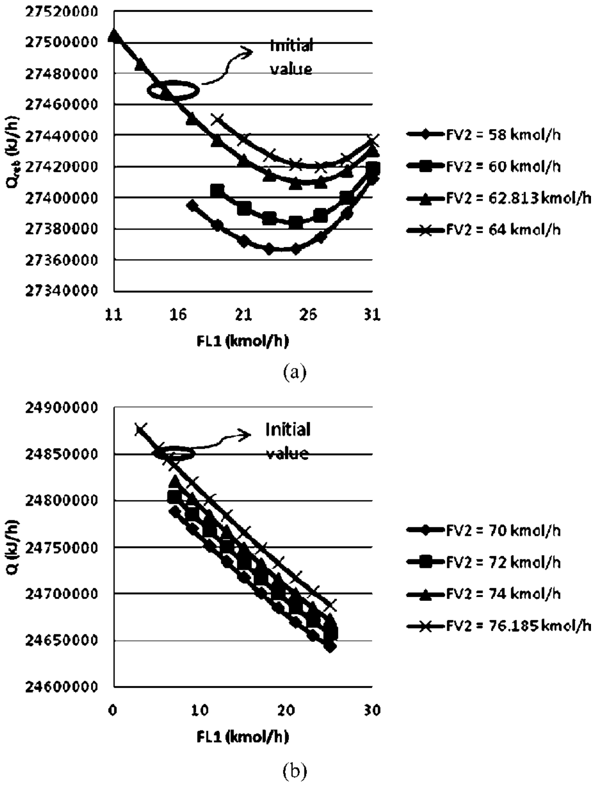

(a)

(b)

Figure 11. Optimization curves for interlinking flows in the RDWC: (a) design obtained by method 1; (b) design obtained by method 2.

theless, both of the reactive dividing wall columns have the same number of stages; notice that the difference between them is only the definition of the interlinking stages. Therefore, according to these results, the design problem of a reactive thermally coupled system seems to be very sensitive to the changes in any of the design variables (number of reactive stages, location of both the side stream and the interlinking stages) and care must be taken when solving this kind of problem.

Table 6. Designs Obtained from the Two Solution Methods, RTCDS

	method 1	method 2
N_1	7	7
N_2	3	2
N_3	1	1
$N_{MC,calc}$	10	9
$N_{MC,total}$	12	11
N_{sr}	1	1
N_{reac}	9−11	9−10
interlinking stages	8	8
R_{col}	1.421	0.01
FV (kmol/h)	181.788	181.009
$Q_{reb,sim}$ (kJ/h)	42 626 674.5	75 930 163.3

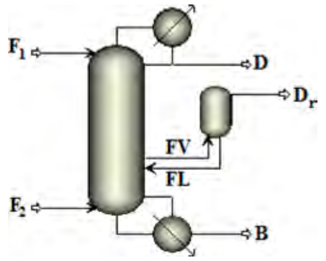

Figure 12. System alternative to RTCDS.

The values for design variables calculated for the RTCDS are presented in Table 6. The number of stages needed for the side rectifier is equal to 1, which means that the separation is easy. Given that result, for simulation purposes, an alternative system including a main column with a flash vaporizer attached instead of the side rectifier was tested. The system is presented in Figure 12. Purities are specified as 91.29 mass % for methyl oleate, 99 mol % for water, and 89.9 mol % for methanol. For this system, high energy requirements can be observed in Table 6, especially for the design obtained by method 2 (RTCDS2). Then, a sensitivity analysis with respect to the main design variables was also performed, trying to improve the designs obtained through our approach. Figure 13 shows the changes in energy requirements against changes in the location of the interlinking flow. When the interlinking streams are located near the bottom of the column, the heat duty is reduced. Figure 14 presents the results when the numbers of reactive and nonreactive stages are modified; energy requirements are considerably reduced if one reactive stage is added to the

Table 5. Final Designs Obtained from the Two Initial Optimal Solutions, RDWC

	RDWC1		RDWC2		
	prefractionator	main column	prefractionator	main column	RDC1
N	5	12	4	12	12
R_{col}	0.6564	1.5640	0.1787	1.3032	1.5278
Q_{cond} (kJ/h)	0	29 600 659.0	0	26 758 629.0	29 206 313
Q_{reb} (kJ/h)	0	27 468 663.3	0	24 845 934.9	27 099 117.7
side stream stage	–	10	–	10	10
reactive stages	–	8−11	–	8−11	8−11
conversion (%)	–	99.95	–	99.97	99.97
interlinking stages	1, 5	5, 10	1, 4	5, 9	–
FV2 (kmol/h)	–	62.813	–	76.185	–
FL1 (kmol/h)	–	14.982	–	6.214	–
T_d (K)	506.94	332.04	506.29	332.03	332.04
T_b (K)	510.16	559.94	507.32	561.83	559.92
P_d (bar)	69.65	69.65	69.65	69.65	69.65
P_b (bar)	69.65	70.34	69.65	70.34	70.34

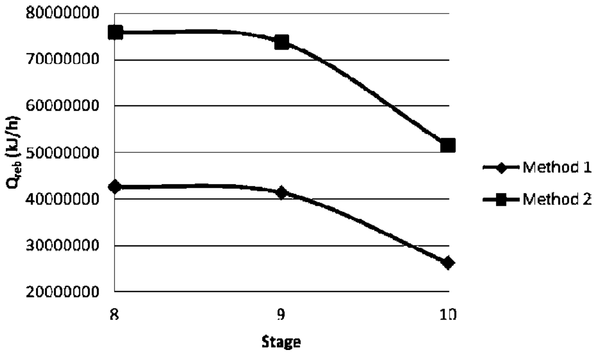

Figure 13. Variation of energy requirements with respect to changes in the interlinking stream withdrawal stage (RTCDS).

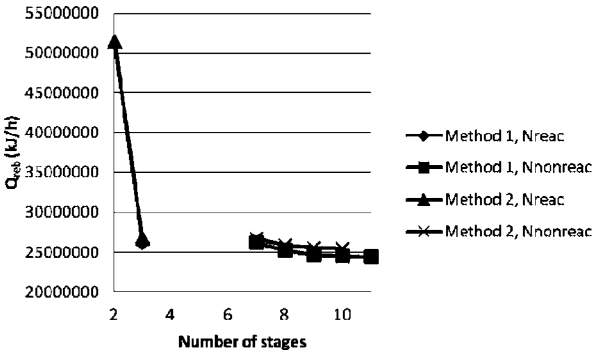

Figure 14. Variation of energy requirements with respect to changes in the number of reactive and nonreactive stages (RTCDS).

RTCDS2. No more stages could be added due to convergence problems. Furthermore, an increment in N_{reac} was not possible in the case of the RTCDS1 (a single point appears for reactive stages in the design obtained by using method 1). Notice that energy requirements of both of the RTCDS systems become almost the same after one additional reactive stage has been incorporated to the RTCDS2 and the RTCDS1 remains unchanged. In addition, a slight reduction in energy requirements is observed in both cases when the number of nonreactive stages is increased. Changes in the interlinking stream flow rate are feasible, but they were avoided to maintain the quality of the stream leaving the side vaporizer within specifications. Thus, the FV flow rate was fixed at the value obtained by the optimization method. The final designs for the RTCDS are presented in Table 7. In this case only the data for the main column are presented. The side vaporizer operates at 7 MPa and 229 °C, with a vapor fraction of approximately 0.96. Again, a reactive distillation column was used to contrast the performance of the thermally coupled designs. Here, the RDC (RDC2) was designed considering the total number of stages of the thermally coupled sequence, i.e., the number of stages on the main column plus an additional stage for the side vaporizer. Both of the modified designs for the RTCDS are basically the same, and their energy requirements are quite similar. Furthermore, the equivalent reactive distillation scheme presents considerably higher energy requirements when compared to the RTCDS configurations.

For the purpose of comparison, Table 8 presents the results obtained for the design of the RDWC using both the shortcut method and the rigorous simulation; similarly, a comparison for the RTCDS is shown in Table 9. The optimal designs obtained for the RDWC by the shortcut method and those modified by the rigorous simulation are quite similar, and the main difference corresponds to the location of the side stream. Nevertheless, small changes in that variable allow reductions of about 48% (method 1) and 46% (method 2) in the energy demand. For the RTCDS, small variations in the location of the interlinking stage also allow reductions of 38% (method 1) and 65% (method 2) in the reboiler duty.

Table 7. Final Designs Obtained from the Two Initial Optimal Solutions, RTCDS

	RTCDS1, main column	RTCDS2, main column	RDC2
N	12	12	13
R_{col}	1.1898	1.2910	2.6220
Q_{cond} (kJ/h)	24 541 002.0	24 687 013.2	40 822 693.0
Q_{reb} (kJ/h)	26 227 225.0	26 762 709.2	38 934 856.3
side stream stage	–	–	10
reactive stages	9–11	9–11	10–12
conversion (%)	99.86	99.88	99.06
interlinking stages	10	10	–
FV (kmol/h)	181.788	181.009	–
T_d (K)	332.02	332.04	332.04
T_b (K)	568.10	568.26	568.32
P_d (bar)	69.65	69.65	69.65
P_b (bar)	70.34	70.34	70.34

Table 8. Comparison between the Obtained Designs for the RDWC

	RDWC1		RDWC2	
	shortcut	rigorous	shortcut	rigorous
N_{pre}	5	5	4	4
N_{MC}	11	12	9	12
N_{reac}	3	4	3	4
interlinking stages	4, 9	5, 10	4, 8	5, 9
side stream stage	7	10	7	10
R_{col}	1.027	1.564	1.214	1.303
FL1 (kmol/h)	14.982	14.982	6.214	6.214
FV2 (kmol/h)	62.813	62.813	76.185	76.185
Q_{reb} (kJ/h)	53 083 486.4	27 468 663.3	46 344 109.2	24 845 934.9

Table 9. Comparison between the Obtained Designs for the RTCDS

	RTCDS1		RTCDS2	
	shortcut	rigorous	shortcut	rigorous
N_{MC}	12	12	11	12
N_{sr}	1	1	1	1
N_{reac}	3	3	2	3
interlinking stages	8	10	8	10
R_{col}	1.421	1.1898	0.01	1.291
FV (kmol/h)	181.788	181.788	181.009	181.009
Q_{reb} (kJ/h)	42 626 674.5	26 227 225.0	75 930 163.3	26 762 709.2

The global mass and energy balances for the initial designs and the optimized designs with the lowest energy requirements are shown in Table 10; the index "i" represents the initial, nonoptimized designs. Since the different systems are designed to accomplish purity constraints, the material balances do not

Table 10. Mass and Energy Balances for the Initial and Optimal Cases

	RDC$_i$	RD1	RPC$_i$	RDWC2	RTCDS$_i$	RTCDS1
F_1 (kmol/h)	267.63	267.63	267.63	268.76	267.63	267.63
F_2 (kmol/h)	412.77	412.77	412.77	412.77	412.77	412.77
D (kmol/h)	265.81	266.65	265.81	268.39	250.15	251.92
S/D_r (kmol/h)	158.76	159.32	158.76	161.48	174.63	174.97
B (kmol/h)	255.83	254.43	255.83	251.65	255.62	253.51
FV1/FV (kmol/h)	–	–	20.02	64.98	181.44	181.79
FL1/FL (kmol/h)	–	–	31.75	6.21	6.80	6.82
FV2 (kmol/h)	–	–	31.75	76.19	–	–
FL2 (kmol/h)	–	–	43.48	15.03	–	–
$H - F_1$ (kJ/kmol)	−472 670	−472 670	−472 670	−472 260	−472 670	−472 670
$H - F_2$ (kJ/kmol)	−193 750	−193 750	−193 750	−193 750	−193 750	−193 750
$H - D$ (kJ/kmol)	−286 910	−287 900	−287 560	−287 850	−287 920	−287 930
$H - S/D_r$ (kJ/kmol)	−239 140	−234 860	−236 420	−235 910	−223 030	−203 430
$H - B$ (kJ/kmol)	−370 930	−372 370	−371 090	−371 380	−381 280	−38 1980
H − FV1/FV (kJ/kmol)	–	–	−217 380	−20 1690	−204 230	−203 680
H − FL1/FL (kJ/kmol)	–	–	−298 430	−325 850	−246 670	−236 180
H − FV2 (kJ/kmol)	–	–	−207 330	−204 270	–	–
H − FL2 (kJ/kmol)	–	–	−269 220	−257 270	–	–

differ considerably for the product streams, and the differences in the energy requirements for the analyzed systems depend mainly on the energetic contents of the interlinking streams. H represents the molar enthalpy of each of the corresponding streams listed in Table 10. Finally, a comparison among the energy requirements for the initial designs and the optimized designs is presented in Table 11. The reference for the calculation of the percentage of reduction is the initial design for a reactive distillation column.[39] It is clear that all of the optimized systems (RDWC1, RDWC2, RTCDS1, and RTCDS2) present considerably lower energy requirements than the initial systems. The case of the RDC2 system is interesting, since its heat duty is even higher than that of the initial system; this result may indicate that designing an RDC based on the RTCDS system is not appropriate, perhaps due to the difference in the side stream phase.

Table 11. Comparison of Energy Requirements for the Initial and Optimized Designs

design	Q_{reb} (kJ/h)	reduction in energy requirements (%)
RDC$_i$	35 053 076.2	0
RPC$_i$	31 680 293.7	9.62
RTCDS$_i$	27 745 638.2	20.85
RDC1	27 099 117.7	22.69
RDWC1	27 468 663.3	21.64
RDWC2	24 845 934.9	31.84
RDC2	38 934 856.3	11.07
RTCDS1	26 227 225.0	25.18
RTCDS2	26 762 709.2	23.65

According to our results, the design and optimization methodology allows obtaining designs for thermally coupled reactive distillation systems with lower energy demands than those of the initial designs obtained by pure parametric analysis. It is clear that the use of the FUG equations to design the columns is questionable because such equations were originally developed for conventional distillation, whereas in reactive distillation different phenomena such as mixing and diffusion controlled reactions may modify the performance of the process. Nevertheless, since the proposed method only considers global material and energy balances, it could be expected that such phenomena have their main effect on the internal profiles, not on the external data required for the calculations. Furthermore, the reaction takes place in a single liquid phase with low mass transfer resistance and high reaction rate, so the mentioned effects can be expected to be lower. Of course, further analysis is needed to determine if such considerations are acceptable for reactions limited by equilibrium or by mass transfer. For the case study presented here, the FUG equations have been shown to be useful to determine an appropriate number of stages for the nonreactive sections but, for the reactive sections, the number of stages is lower than the one required. Nevertheless, very small changes, such as increasing the number of stages by just one, allow obtaining the desired purities and conversions. Thus, the FUG method may underestimate the design of the reactive section, but only slight modifications were needed to achieve the expected performance.

On the other hand, it has been noticed that the energy demand for the different analyzed systems has been considerably reduced when manipulating the location of the side stream. This occurs because it has been assumed in the design methodology that the side stream is located on the boundary region between the reactive and nonreactive sections; thus the NLP solution presents designs which fulfill such a constraint. Nevertheless, according to the sensitivity analysis, the side stream must be located inside the reactive section of the column to achieve low thermal duty.

As expected, for the RTCDS, the results show that method 1 allows obtaining better designs in terms of thermal duty than method 2. However, for the RDWC, the results of method 2 are better than those of method 1. In general, simultaneous solution (method 1) should result in better designs. Nevertheless, since the number of stages in method 1 is considered to be a continuous variable in the optimization strategy, and given the high sensitivity of the system to small changes in the structure, we speculate that the NLP solution for the design equations predicts an inappropriate location for the interlinking stages in the RDWC; this may be due to the fact that shortcut equations lack significant gradient information that could lead the design to the actual optimal point. As shown in Table 4, even a small change in the location of the interlinking stages may rise to higher energy requirements. Notice that this effect does not impact the results for the RTCDS, where the interlinking stage has been fixed at the boundary region between the reactive and nonreactive sections.

8. CONCLUSIONS

A simplified design method for thermally coupled reactive distillation systems has been presented. The design is based on the FUG equations; the use of the FUG equations to design the columns is of course questionable because such equations were originally developed for conventional distillation. The potential effect of phenomena such as mixing and diffusion controlled reactions is being neglected. However, for the case study presented here, the FUG equations have shown to be useful to determine an appropriate number of stages for the nonreactive sections and, for the reactive sections, only slight modifications were needed to achieve the expected performance.

The optimization strategy aims to minimize energy requirements by adjusting interlinking streams and the reflux ratios. Two solution methods have been proposed. One of the main complexities found when solving the complete system of equations in method 1 occurs in the calculation of the Underwood roots. On the other hand, different designs are obtained by both solution methods, which is natural because method 1 is a simultaneous approach and method 2 is a sequential approach. The designs obtained by both of the proposed methods have been studied through a sensitivity analysis, aiming to improve the performance of the configurations and correct the values of the design variables (if needed).

It has been found that, for the RDWC, high energy requirements are obtained when the side stream is assumed to be located at the boundary region between the nonreactive zone and the reactive zone. Thus, the side stream must be located in the reactive zone. The same occurs for the interlinking flow on the RTCDS.

As mentioned above, the number of reactive stages calculated by the FUG equations results slightly lower than the required number to obtain high conversions with low heat duty. However, only one additional reactive stage was necessary in all of the cases to achieve low thermal duty for the reboiler. In the case of the interlinking flows on the RDWC, changes in energy requirements, when the flow rates of FL1 and FV2 are modified, are not significant. The final designs obtained do show a significant reduction in energy requirements for both systems, RDWC and RTCDS, when compared to the initial designs.

Thus, the proposed methodology allows obtaining proper designs for the intensified systems under analysis, achieving the desired purities and conversions with potential low heat duty. The method has been tested with a reaction occurring at a high reaction rate; further analysis is required for reactions limited by chemical equilibrium. Furthermore, since the reaction under analysis occurs at high temperature and pressure, additional analysis is also required to determine if such a system can be successfully operated in practice.

■ AUTHOR INFORMATION

Corresponding Author

*E-mail: vicente@iqcelaya.itc.mx. Tel.: (+52) 461 611 7575, ext 156.

Notes

The authors declare no competing financial interest.

■ ACKNOWLEDGMENTS

The authors acknowledge the financial support provided by CONACyT, PROMEP, and DGEST (Mexico).

■ NOMENCLATURE

$d_{i,k}$ [kmol/h] = molar flow rate of component i at the top of section k

$b_{i,k}$ [kmol/h] = molar flow rate of component i at the bottom of section k

D [kmol/h] = total molar flow rate of the distillate of the main column

S [kmol/h] = total molar flow rate of the liquid side stream of the main column

B [kmol/h] = total molar flow rate of the bottom of the main column

D_r [kmol/h] = total molar flow rate of the distillate of the side rectifier in a reactive thermally coupled direct sequence

f_{conv} = molar global conversion

f_{part} = partition factor

F_j [kmol/h] = molar flow rate of feed stream j

F_{kT} [kmol/h] = molar flow rate of pseudofeed stream to section k

h [kJ/kmol] = molar enthalpy of the stream

$h_{rxn,i}$ [kJ/kmol] = molar enthalpy of the reaction, referred to component i

K_{eq} = vapor−liquid equilibrium constant

P_i^{sat} [Pa] = vapor pressure for component i

P [Pa] = total pressure on the system

q_{pfk} = liquid fraction for the pseudofeed stream to section k

Q_{COND} [kJ/h] = thermal energy released in the condenser

Q_{ent} [kJ/h] = total amount of heat entering the system

Q_{out} [kJ/h] = total amount of heat leaving the system

Q_{reb} [kJ/h] = thermal duty in the reboiler

Q_{rxn} [kJ/h] = heat of reaction

$\text{rec}_{d,i,j,k}$ = recovery of component i from feed stream j at the top of section k

$\text{rec}_{b,i,j,k}$ = recovery of component i from feed stream j at the bottom of section k

V [kmol/h] = molar flow rate of the vapor entering the condenser

V_{min} [kmol/h] = minimum vapor flow

x_i = molar composition of component i in the liquid phase

y_i = molar composition of component i in the vapor phase

$y_{Vd,i}$ = molar composition of component i in the vapor entering the condenser

$z_{j,i}$ = molar composition of component i in feed stream j

Greek Symbols

Φ_i = corrected fugacity coefficient

γ_i = activity coefficient for component i

λ_i [kJ/kmol] = enthalpy of vaporization for component i

ν_i = stoichiometric coefficient for component i

ν_{rr} = stoichiometric coefficient for reference component r in the reaction

θ_n = Underwood root for section 1

θ_n' = Underwood root for section 2

θ_n'' = Underwood root for section 3

■ REFERENCES

(1) Agrawal, R.; Fidkowski, Z. T. Are Thermally Coupled Distillation Columns Always More Efficient for Ternary Distillations? *Ind. Eng. Chem. Res.* **1998**, *37*, 3444.

(2) Flores, O. A.; Cárdenas, J. C.; Hernández, S.; Rico-Ramírez, V. Thermodynamic Analysis of Thermally Coupled Distillation Sequences. *Ind. Eng. Chem. Res.* **2003**, *42*, 5940.

(3) Triantafyllou, C; Smith, R. The Design and Optimization of Fully Thermally Coupled Distillation Columns. *Trans. Inst. Chem. Eng.* **1992**, *70A*, 118.

(4) Petlyuk, F. B.; Platonov, V. M.; Slavinskii, D. M. Thermodynamically Optimal Method for Separating Multicomponent Mixtures. *Int. Chem. Eng.* **1965**, *5* (3), 555.

(5) Stupin, W. J.; Lockhart, F. J. Thermally Coupled Distillation—A Case History. *Chem. Eng. Prog.* **1972**, *68* (10), 71.

(6) Tedder, D. W.; Rudd, D. F. Parametric Studies in Industrial Distillation: Part I. Design Comparisons. *AIChE J.* **1978**, *24*, 303.

(7) Glinos, K.; Malone, F. Optimality Regions for Complex Column Alternatives in Distillation Systems. *Chem. Eng. Res. Des.* **1988**, *66*, 229.

(8) Amminudin, K. A.; Smith, R.; Thong, D. Y.-C.; Towler, G. P. Design and Optimization of Fully Thermally Coupled Distillation Columns. Part 1: Preliminary Design and Optimization Methodology. *Trans. Inst. Chem. Eng.* **2001**, *79* (Part A), 701.

(9) Hernández, S.; Jiménez, A. Controllability Analysis of Thermally Coupled Distillation Systems. *Ind. Eng. Chem. Res.* **1999**, *38*, 3957.

(10) Jiménez, A.; Hernández, S.; Montoy, F. A.; Zavala-García, M. Analysis of Control Properties of Conventional and Nonconventional Distillation Sequences. *Ind. Eng. Chem. Res.* **2001**, *40*, 3757.

(11) Segovia-Hernández, J. G.; Hernández, S.; Jiménez, A. Control Behaviour of Thermally Coupled Distillation Sequences. *Tran. Inst. Chem. Eng.* **2002**, *80*, 783.

(12) Segovia-Hernández, J. G.; Hernández, S.; Rico-Ramirez, V.; Jiménez, A. A Comparison of the Feedback Control Behaviour Between Thermally Coupled and Conventional Distillation Schemes. *Comput. Chem. Eng.* **2004**, *28*, 811.

(13) Dejanovic, I.; Matijasevic, Lj.; Olujic, Z. Dividing Wall Column—A Breakthrough Towards Sustainable Distilling. *Chem. Eng. Process.* **2010**, *49*, 559.

(14) Olujic, Z.; Jödecke, M.; Shilkin, A.; Schuch, G.; Kaibel, B. Equipment improvement trends in distillation. *Chem. Eng. Process.* **2009**, *48* (6), 1089.

(15) van Diggelen, R. C.; Kiss, A. A.; Heemink, A. W. Comparison of Control Strategies for Dividing-Wall Columns. *Ind. Eng. Chem. Res.* **2010**, *49*, 288.

(16) Kiss, A. A.; Bildea, C. S. A Control Perspective on Process Intensification in Dividing-Wall Columns. *Chem. Eng. Process.* **2011**, *50*, 281.

(17) Kiss, A. A.; Pragt, J. J.; Van Strien, C. J. G. Reactive Dividing-Wall Columns—How to Get More with Less Resources? *Chem. Eng. Commun.* **2009**, *196*, 1366.

(18) Taylor, R.; Krishna, R. Modelling Reactive Distillation. *Chem. Eng. Sci.* **2000**, *55*, 5183.

(19) Buzad, G.; Doherty, M. F. Design of Three-Component Kinetically Controlled Reactive Distillation Columns Using Fixed-Points Methods. *Chem. Eng. Sci.* **1994**, *49* (12), 1947.

(20) Buzad, G.; Doherty, M. F. New Tools for the Design of Kinetically Controlled Reactive Distillation Columns for Ternary Mixtures. *Comput. Chem. Eng.* **1995**, *19* (4), 395.

(21) Giessler, S.; Danilov, R. Y.; Pisarenko, R. Y.; Serafimov, L. A.; Hasebe, S.; Hashimoto, I. Feasibility Study of Reactive Distillation Using the Analysis of the Statics. *Ind. Eng. Chem. Res.* **1998**, *37*, 4375.

(22) Barbosa, D.; Doherty, M. F. The Simple Distillation of Homogeneous Reactive Mixtures. *Chem. Eng. Sci.* **1988**, *43* (3), 541.

(23) Espinosa, J.; Aguirre, P.; Pérez, G. Some Aspects in the Design of Multicomponent Reactive Distillation Columns Including Non-reactive Species. *Chem. Eng. Sci.* **1995**, *50* (3), 469.

(24) Bessling, B.; Schembecker, G.; Simmrock, K. H. Design of Processes with Reactive Distillation Line Diagrams. *Ind. Eng. Chem. Res.* **1997**, *36*, 3032.

(25) Groemping, M.; Dragomir, R. M.; Jobson, M. Conceptual Design of Reactive Distillation Columns Using Stage Composition Lines. *Chem. Eng. Process.* **2004**, *43*, 369.

(26) Sánchez-Daza, O.; Pérez-Cisneros, E. S.; Bek-Pedersen, E.; Gani, R. Graphical and Stage-to-Stage Methods for Reactive Distillation Column Design. *AIChE J.* **2003**, *49* (11), 2822.

(27) Stichlmair, J.; Frey, T. Mixed-Integer Nonlineal Programming Optimization of Reactive Distillation Processes. *Ind. Eng. Chem. Res.* **2001**, *40*, 5978.

(28) Jackson, J. R.; Grossmann, I. E. A Disjunctive Programming Approach for the Optimal Design of Reactive Distillation Columns. *Comput. Chem. Eng.* **2001**, *25*, 1661.

(29) Cardoso, M. F.; Salcedo, R. L.; Feyo de Azevedo, S.; Barbosa, D. Optimization of Reactive Distillation Processes with Simulated Annealing. *Chem. Eng. Sci.* **2000**, *55*, 5059.

(30) Cheng, J. K.; Lee, H. Y.; Huang, H. S.; Yu, C. C. Optimal Steady-State Design of Reactive Distillation Processes Using Simulated Annealing. *J. Taiwan Inst. Chem. Eng.* **2009**, *40*, 188−196.

(31) Panjwani, P.; Schenk, M.; Georgiadis, M. C.; Pistikopoulos, E. N. Optimal Design and Control of a Reactive Distillation System. *Eng. Optim.* **2005**, *37* (7), 733.

(32) Seferlis, P.; Grievink, J. Optimal Design and Sensitivity Analysis of Reactive Distillation Units Using Collocation Models. *Ind. Eng. Chem. Res.* **2001**, *40*, 1673.

(33) Dalaouti, N.; Seferlis, P. A Unified Modeling Framework for the Optimal Desgn and Dynamic Simulation of Staged Reactive Separation Processes. *Comput. Chem. Eng.* **2006**, *30*, 1264.

(34) Damartzis, T.; Seferlis, P. Optimal Design of Staged Three-Phase Reactive Distillation Columns Using Nonequilibrium and Orthogonal Collocation Models. *Ind. Eng. Chem. Res.* **2010**, *49*, 3275−3285.

(35) Barroso-Muñoz, F. O.; S. Hernández, S.; Segovia-Hernández, J. G.; Hernández-Escoto, H.; Aguilera-Alvarado, A. F. Thermally Coupled Distillation Systems: Study of an Energy-Efficient Reactive Case. *Chem. Biochem. Eng. Q.* **2007**, *21* (2), 115.

(36) Mueller, I.; Kenig, E. Y. Reactive Distillation in a Dividing Wall Column: Rate-Based Modeling and Simulation. *Ind. Eng. Chem. Res.* **2007**, *46*, 3709.

(37) Hernández, S.; Sandoval-Vergara, R.; Barroso-Muñoz, F. O.; Murrieta-Dueñas, R.; Hernández-Escoto, H.; Segovia-Hernández, J. G.; Rico-Ramirez, V. Reactive Dividing Wall Distillation Columns. *Chem. Eng. Process.* **2009**, *48*, 250.

(38) Gomez-Castro, F. I.; Rico-Ramirez, V.; Segovia-Hernandez, J. G.; Hernandez, S. Feasibility Study of a Thermally Coupled Reactive Distillation Process for Biodiesel Production. *Chem. Eng. Process.* **2010**, *49*, 262.

(39) Gomez-Castro, F. I.; Rico-Ramirez, V.; Segovia-Hernández, J. G.; Hernandez-Castro, S. Esterification of Fatty Acids in a Thermally Coupled Reactive Distillation Column by the Two-Step Supercritical Methanol Method. *Chem. Eng. Res. Des.* **2011**, *89*, 480−490.

(40) Kiss, A. A.; Omota, F.; Dimian, A. C.; Rothenberg, G. The Heterogeneous Advantage: Biodiesel by Catalytic Reactive Distillation. *Top. Catal.* **2006**, *40*, 141.

(41) Kiss, A. A.; Dimian, A. C.; Rothenberg, G. Biodiesel by Catalytic Reactive Distillation Powered by Metal Oxides. *Energy Fuels* **2008**, *22*, 598.

(42) da Silva, N. de L.; Garcia Santander, C. M.; Batistella, C. B.; Maciel Filho, R.; Wolf Maciel, M. R. Biodiesel Production from Integration Between Reaction and Separation System: Reactive Distillation Process. *Appl. Biochem. Biotechnol.* **2010**, *161*, 245.

(43) Kiss, A. A. Separative Reactors for Integrated Production of Bioethanol and Biodiesel. *Comput. Chem. Eng.* **2010**, *34*, 812.

(44) Smith, J. M.; Van Ness, H. C.; Abbott, M. M. *Introduction to Chemical Engineering Thermodynamics*, 6th ed.; McGraw-Hill: New York, 2001; in SI units.

(45) Sotudeh, N.; Shahraki, B. H. A Method for the Design of Divided Wall Columns. *Chem. Eng. Technol.* **2007**, *30* (9), 1284.

(46) Halvorsen, I. J.; Skogestad, S. Minimum Energy Consumption in Multicomponent Distillation. 2. Three-Product Petlyuk Arrangements. *Ind. Eng. Chem. Res.* **2003**, *42*, 605−615.

(47) Miranda-Galindo, E. Y.; Segovia-Hernández, J. G.; Hernández, S.; Gutiérrez-Antonio, C.; Briones-Ramírez, A. Reactive Thermally Coupled Distillation Sequences: Pareto Front. *Ind. Eng. Chem. Res.* **2011**, *50*, 926−938.

(48) Shah, V. H.; Agrawal, R. Are All Thermal Coupling Links between Multicomponent Distillation Columns Useful from an Energy Perspective? *Ind. Eng. Chem. Res.* **2011**, *50*, 1770−1777.

(49) Minami, E.; Saka, S. Kinetics of Hydrolysis and Methyl Esterification for Biodiesel Production in Two-Step Supercritical Methanol Process. *Fuel* **2006**, *85*, 2479.

(50) Saka, S. NEDO Biodiesel Production Process by Supercritical Methanol Technologies. Presented at the The 2nd Joint International Conference on Sustainable Energy and Development, Bangkok, Thailand, November 2006.

(51) Saka, S.; Kusdiana, D. Biodiesel Fuel from Rapeseed Oil as Prepared in Supercritical Methanol. *Fuel* **2001**, *80*, 225.